

A Refined Model for the Somatostatin Pharmacophore: Conformational Analysis of Lanthionine–Sandostatin Analogs

Giuseppe Melacini, Qin Zhu,[†] George Ösapay,[‡] and Murray Goodman*

Department of Chemistry and Biochemistry, University of California at San Diego, La Jolla, California 92093-0343

Received December 17, 1996[©]

We report the conformational analysis of a series of analogs of sandostatin (octreotide, D-Phe¹-c[Cys²-Phe³-D-Trp⁴-Lys⁵-Thr⁶-Cys⁷]-Thr⁸-ol) using ¹H NMR spectroscopy and molecular modeling. Two active compounds in which the disulfide group is replaced by a monosulfide (lanthionine) bridge (D-Phe¹-c[Ala^L²-Phe³-D-Trp⁴-Lys⁵-Thr⁶-Ala^L⁷]-Thr⁸-ol and D-Phe¹-c[Ala^L²-Phe³-D-Trp⁴-Lys⁵-Thr⁶-Ala^L⁷]-Thr⁸-NH₂, where Ala^L denotes each of the lanthionine amino acid ends linked by the monosulfide bridge) show different mSSTR2b/rSSTR5 receptor selectivities as compared to sandostatin. These new results have enabled us to reveal features of the somatostatin pharmacophore common to the model previously proposed in our laboratory on the basis of main chain and side chain chiral methylation studies. In addition, our studies provide new insight into the role of the disulfide bridge and of Thr⁸ in binding potency. We also show that the lanthionine group is a good mimetic of β -VI turns and can be incorporated in sandostatin analogs maintaining the essential secondary structural features of sandostatin. These results facilitate the design of new sandostatin peptidomimetics.

Introduction

The cyclic tetradecapeptide hormone somatostatin was first known as an inhibitor of the release of growth hormone.¹ Later, somatostatin was also shown to inhibit the release of glucagon, insulin, gastrin, and secretin.^{2–5} Furthermore, somatostatin plays a role in neural transmission as indicated by its effects on neurons⁶ and its distribution in the brain and spinal cord.^{7,8}

Structure–activity studies have resulted in the synthesis of several highly bioactive analogs of somatostatin, including the cyclic hexapeptide c[Pro²-Phe³-D-Trp⁴-Lys⁵-Thr⁶-Phe⁷], denoted as L-363-301 (we maintain the same residue numbering which is used for the octreotide sandostatin **I**).⁹ The synthesis and conformational analysis of main chain and side chain chiral methylated analogs of compound L-363-301 allowed us to propose a model for somatostatin pharmacophores. In this model the peptide backbone adopts a β -II' turn about residues D-Trp⁴-Lys⁵ and a β -VI turn about the Phe⁷-Pro² bridging region.^{10,11} The overall structure is folded about the Phe³ and Thr⁶ residues, which assume a C₇ conformation for their ϕ and ψ torsions. The model requires also that the D-Trp⁴ side chain assumes the *trans* rotamer, while the Lys⁵ side chain adopts the *gauche* (–) (*g*[–]) rotamer, thus allowing a close proximity between these two side chains. The Phe⁷ side chain prefers the *trans* rotamer in the proposed “bioactive conformation”, while no exact topochemical requirement for binding activity is identified for Phe³ although the aromatic group at position 3 is important for binding activity.¹¹

We now investigate the somatostatin pharmacophore using chemical modifications of D-Phe¹-c[Cys²-Phe³-D-

Trp⁴-Lys⁵-Thr⁶-Cys⁷]-Thr⁸-ol,¹² known as sandostatin or octreotide (Table 1, compound **I**). In sandostatin **I** a disulfide bridge is used to stabilize the conformation of the bioactive sequence Phe-D-Trp-Lys-Thr. Sandostatin also adopts a β -II' turn spanning residues D-Trp⁴ and Lys⁵. The β -II' turn of sandostatin is part of a β -sheet conformation. Backbone modifications or isosteric replacements which do not conserve this backbone conformation lead to compounds inactive as agonists of somatostatin.¹³ In order to introduce conformational constraints, we have designed and synthesized a series of sandostatin analogs¹⁴ in which the disulfide bridge has been replaced by a monosulfide bridge (lanthionine bridge), a structural component of numerous naturally occurring molecules such as nisin, subtilin, and epidermin.¹⁵

In this paper we report the conformational analysis by 1D and 2D ¹H NMR experiments and molecular modeling of a series of cyclic analogs of sandostatin including two lanthionine octamers with different C-terminal groups (Table 1, compounds **II** and **III**), one disulfide, and one lanthionine heptamer in which the Thr⁸-ol is missing (Table 1, compounds **IV** and **V**).¹⁴ The conformational features of these analogs are compared to the previously characterized conformations of sandostatin¹⁶ and of compound L-363-301.¹¹ These comparisons reveal pharmacophore features also found in the model for somatostatin binding activity based on main chain and side chain chiral methylation studies¹¹ and provide new insight into the biological role of the bridging region and of Thr⁸-ol.

Materials and Methods

NMR Spectroscopy. The samples were synthesized as previously described¹⁴ and were dissolved and then lyophilized in DMSO-*d*₆ purchased from Merck Sharp and Dohme Canada Ltd. The dry samples were redissolved in DMSO-*d*₆ at concentrations of approximately 6 mM and degassed by the freeze–pump–thaw method. All ¹H NMR spectra were measured on a Bruker AMX 500 spectrometer operating at 500 MHz. The one-dimensional spectra contain 16K data points

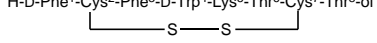
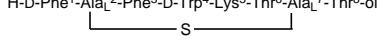
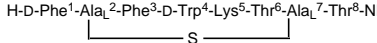
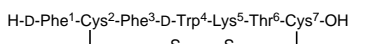
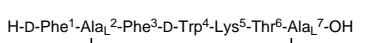
* Author to whom correspondence should be addressed.

[†] Present address: Department of Biochemistry, Purdue University, West Lafayette, IN 47907.

[‡] Present address: College of Medicine, University of California Irvine, Irvine, CA 92717-4800.

[©] Abstract published in *Advance ACS Abstracts*, June 15, 1997.

Table 1. Sandostatin Analogs Studied^a

no.	analog	sequence	IC ₅₀ (nM)		
			mSSTR2b	rSSTR5	hSSTR5
I	sandostatin ^b	H-D-Phe ¹ -Cys ² -Phe ³ -D-Trp ⁴ -Lys ⁵ -Thr ⁶ -Cys ⁷ -Thr ⁸ -ol 	0.28	1.04	0.77
II	lanthionine octamer-ol ^c	H-D-Phe ¹ -Ala ^L ² -Phe ³ -D-Trp ⁴ -Lys ⁵ -Thr ⁶ -Ala ^L ⁷ -Thr ⁸ -ol 	13.13	1.29	4.17
III	lanthionine octamer-NH ₂ ^c	H-D-Phe ¹ -Ala ^L ² -Phe ³ -D-Trp ⁴ -Lys ⁵ -Thr ⁶ -Ala ^L ⁷ -Thr ⁸ -NH ₂ 	15.60	5.50	4.92
IV	disulfide heptamer-OH	H-D-Phe ¹ -Cys ² -Phe ³ -D-Trp ⁴ -Lys ⁵ -Thr ⁶ -Cys ⁷ -OH 	13.62	10.63	10.95
V	lanthionine heptamer-OH ^c	H-D-Phe ¹ -Ala ^L ² -Phe ³ -D-Trp ⁴ -Lys ⁵ -Thr ⁶ -Ala ^L ⁷ -OH 	> 1000	500	N/D

^a The synthesis of these compounds is reported in ref 14. ^b The conformational analysis of sandostatin is reported in ref 16. ^c Ala^L denotes each of the lanthionine amino acids linked by the monosulfide bridge.

with a spectral width of 6500 Hz. The 1D spectra acquired at temperatures between 300 and 320 K were used to measure the amide resonance temperature coefficients. 2D spectra were acquired at 300 K. The total correlation spectroscopy (TOCSY) experiments were performed using the MLEV-17 sequence and the time proportional phase increment.^{17,18} A mixing time of 75 ms with a spin-locking field of 10 kHz was employed. The rotating frame nuclear Overhauser (ROESY) experiments¹⁹ were carried out with mixing times of 100, 200, and 300 ms. A spin-locking field of 2.5 kHz was used. The TOCSY and ROESY experiments were obtained using 2K data points in the f_2 domain and 256 points in the f_1 domain. Zero-filling was applied in the f_1 and f_2 domains to obtain a matrix of 2K × 2K data points. The DQF-COSY experiments were acquired using 4K data points in the f_2 domain in order to have higher digital resolution. Multiplication with a phase-shifted sinebell function was employed to enhance the spectra.

Using TOCSY spectra all spin systems were identified. The ROESY spectra were employed for the sequential assignment²⁰ and the identification of the aromatic spin systems through the connectivities with the remainder of the residues. Chemical shifts were measured using DMSO-*d*₆ ($\delta = 2.49$ ppm) as an internal standard. The observed signals of nonoverlapping C ^{β} H resonances were stereospecifically assigned to their respective C ^{β} H protons following the procedure described by Yamazaki et al.²¹ The $J_{\text{NH-H}\alpha}$ and $J_{\text{H}\alpha\beta}$ coupling constants were obtained by 1D spectra and by sections of cross peaks from the resolution-enhanced 4K × 2K DQF-COSY spectra. The ROESY cross peak volumes were calibrated against the distance between the indole and H2 protons of D-Trp⁴ using the isolated spin pair approximation. On the basis of the comparison with other known distances, an error of approximately ± 0.5 Å was estimated. Consequently, the upper and lower distance constraints were set to the measured distance ± 0.5 Å, respectively.

Molecular Modeling. The structural NMR refinement protocol included distance geometry, energy minimizations, restrained simulated annealing, and cluster analysis. The distance geometry (DG) program DGII was used to generate structures consistent with the distance constraints derived from NOEs. The ϕ torsional angles and hydrogen-bonding patterns of these structures were compared with the values derived from NMR measurements. A Karplus-type equation²² was used to compute the ϕ torsion values consistent with the measured $J_{\text{NH-H}\alpha}$ coupling constants, and an error of $\pm 30^\circ$ was tolerated. In the case of the hydrogen bond based selection, structures were retained in which NH protons with a temperature coefficient > -2 ppb/K²³ donate at least one hydrogen bond. Structures not consistent with these experimental constraints were discarded. The remaining structures were subjected to a restrained simulated annealing protocol.

Molecular dynamics (MD) and mechanics calculations were carried out *in vacuo* employing the DISCOVER program²⁴ with

the CVFF force field, and the NOE restraints were included with a force constant of 15 kcal/(mol Å²). A distance dependent dielectric constant was used to take into account the solvent effects.²⁵ A neutral form of the amino group in the Lys side chain was used in order to be consistent with previous studies.¹¹ A harmonic bond-stretching potential was used. This prevented the bonded atoms from drifting unrealistically far apart because of high-energy nonbonded interactions. During all simulations no cross terms were used because no normal mode analysis was attempted. In all simulations the peptide bonds were kept in the *trans* structure.

Prior to every molecular dynamics simulation the system was equilibrated with 3 ps initialization dynamics. In an attempt to carry out a thorough search of the accessible conformational space, the selected distance geometry structures were first submitted to 10 ps of molecular dynamics at 1000 K with a step size of 1 fs. At regular intervals of 1 ps, conformations were extracted and submitted to a preliminary energy minimization by steepest descent until the maximum derivative was less than 1. Starting from each of these minimized conformations, we proceeded with 10 ps of molecular dynamics at 300 K. Again, at regular intervals of 1 ps, we carried out unrestrained minimizations to generate families of low-energy conformations. For these minimizations the VA09A algorithm was used until the maximum derivative was less than 0.01 kcal/mol.

The simulated annealing protocol led to 100 minimized structures for each structure selected after distance geometry. The resulting conformations were then examined and selected according to their consistency with the NOEs, the $J_{\text{NH-H}\alpha}$ coupling constants and the temperature coefficients. Those structures consistent with the experimental values according to the same criteria used after DG and with energies not higher than 10 kcal/mol compared to the lowest energy were selected²⁶ and used for cluster analysis,²⁷ resulting in preferred conformational families. New conformations were also built combining the clusters found for individual torsions. These new conformations were then minimized and submitted to the same selection criteria discussed above.

Results and Discussion

Backbone Conformations. Using NOEs (Table 2), $J_{\text{NH-H}\alpha}$ coupling constants (Table 3), and temperature coefficients (Table 4) as experimental restraints in our distance geometry and molecular dynamics conformational search, we obtained minimized structures for the sandostatin analogs II–V (Table 1). These structures were then compared with those previously obtained¹⁶ for sandostatin I. The backbone to backbone root mean square deviations (rmsd) between the β -sheet-like conformation of sandostatin I¹⁶ and the structures

Table 2. Summary of the Observed Backbone NOEs^{a,b}

NOE	II	III	IV	V
H _α ¹ -NH ²	m	m	s	s
H _α ² -NH ²	m	m		m
H _α ² -NH ³	s	s	s	s
H _α ² -H _α ⁷	m	s	m	m
H _α ³ -NH ³	m	m	m	m
H _α ³ -NH ⁴	s	s	s	s
H _α ⁴ -NH ⁴	m	s	m	s
H _α ⁴ -NH ⁵	s	s	s	s
H _α ⁵ -NH ⁵	m	m	w	m
H _α ⁵ -NH ⁶	s		m	s
NH ⁵ -NH ⁶	m	m	m	m
H _α ⁶ -NH ⁶	m	m	m	m
H _α ⁶ -NH ⁷	s	s	s	s
NH ⁶ -NH ⁷	m	m	m	m
H _α ⁷ -NH ⁷	m	m	m	m
H _α ⁷ -NH ⁸	s	s		
NH ⁷ -NH ⁸	m	m		
H _α ⁸ -NH ⁸	m	m		

^a For sandostatin (**I**), see ref 16. ^b The NOEs corresponding to distances ≤ 2.5 Å are classified as strong (s); the NOEs corresponding to distances > 2.5 and ≤ 3.5 Å are classified as medium (m); the NOEs corresponding to distances > 3.5 and ≤ 4.5 Å are classified as weak (w). All residues are numbered sequentially as in the octamers, starting from D-Phe¹ and ending with Thr⁸.

obtained for analogs **II–V** are reported in Table 5. The rmsd values for all the analogs (**II–V**) show that their backbones are similar to that of the previously characterized β -sheet-like conformation of sandostatin **I**¹⁶ (Figure 1a,b): a β -II'-like turn stabilized by the Thr⁶ NH-Phe³ C=O hydrogen bond spans residues D-Trp⁴ and Lys⁵ as indicated by the strong H_α⁴-NH⁵ NOEs, by the medium NH⁵-NH⁶ NOEs (Table 2), and by the low-temperature coefficient measured for the Thr⁶ NH resonance (Table 4).²³ The β -sheet-like conformation found for the other parts of the backbone is consistent with the $J_{\text{NH-H}\alpha}$ coupling constants (Table 3) and with the high-temperature coefficients measured for the NH⁴ and the NH⁷ resonances²⁸ (Table 4). These temperature coefficients are in full agreement with the solvent

exposure expected for the NH⁴ and the NH⁷ protons in the antiparallel β -sheet structure (Figure 1).²⁰ The β -sheet-like conformation is also supported by the strong sequential H_α-NH NOEs (see the H_α²-NH³, the H_α³-NH⁴, the H_α⁶-NH⁷, and the H_α⁷-NH⁸ NOEs of Table 2)²⁰ and by the H_α²-H_α⁷ NOE (Table 2). The H_α²-H_α⁷ NOE also indicates that both the lanthionine bridge of analogs **II**, **III**, and **V** and the disulfide bridge of the heptamer **IV** are good mimetics of a β -VI turn for which this type of H_α to H_α NOE is typically observed. The finding that the β -sheet-like conformation is also accessible to the disulfide heptamer (**IV**) is very instructive because it indicates that Thr⁸ is not necessary for a β -sheet-like conformation in the cyclic region. However, the Thr⁸ residue can stabilize the β -sheet-like structure through intramolecular hydrogen bonds, as previously suggested on the basis of theoretical conformational studies.¹²

Our previous investigations on sandostatin **I**¹⁶ have shown that the β -sheet-like conformations are in equilibrium with structures in which the three C-terminal residues adopt a 3₁₀ helix-like fold. Key evidence for the helix-like conformations of sandostatin **I** is the presence of the NH⁶-NH⁷ and NH⁷-NH⁸ NOEs. These NOEs are also observed for the lanthionine octamers **II** and **III** (Table 2), indicating that a similar conformational equilibrium may exist. In addition, the NH⁶-NH⁷ NOE is observed in the heptamers **IV** and **V**, suggesting that in spite of the absence of residue 8 a nascent C-terminally folded structure must still be considered in the conformational equilibrium. Further support for this equilibrium is provided by the high-temperature coefficients measured for the NH³ resonance of the lanthionine octamers **II** and **III** and of the lanthionine heptamer **V**^{23,28} (Table 4). These temperature coefficients are not consistent with the β -sheet-like conformations in which the NH³ is shielded from the solvent by the NH³-C=O⁶ hydrogen bond; however, this hydrogen bond is broken in the helix-like struc-

Table 3. $J_{\text{NH-H}\alpha}$ Coupling Constant and Calculated ϕ^a Values^b

residue	II		III		IV		V	
	$J_{\text{NH-H}\alpha}$ (Hz)	ϕ (deg)	$J_{\text{NH-H}\alpha}$ (Hz)	ϕ (deg)	$J_{\text{NH-H}\alpha}$ (Hz)	ϕ (deg)	$J_{\text{NH-H}\alpha}$ (Hz)	ϕ (deg)
Ala _L ^{2 c}	6.95	39	7.27	43	8.02	-148	8.06	-147
		81		77		-93		-93
		-155		-153				
		-85		-87				
Phe ³	7.33	43	6.95	39	7.49	45	7.69	49
		77		81		74		71
		-153		-155		-152		-150
		-87		-85		-88		-89
D-Trp ⁴	5.14	-97	7.00	-81	4.66	-100	6.60	-85
		-23		-39		-20		-33
		73		85		70		82
		167		155		170		158
Lys ⁵	6.96	39	6.53	35	7.42	44	7.88	53
		81		85		76		67
		-155		-158		-152		-149
		-85		-82		-88		-91
Thr ⁶	7.69	49	7.78	51	8.72	-142	8.24	-146
		71		69		-98		-94
		-150		-150				
		-90		-90				
Ala _L ^{7 c}	8.79	-141	8.30	-146	9.31	-136	8.07	-147
		-99		-94		-104		-93
Thr ⁸	8.80	-141	8.47	-144				
		-99		-96				

^a Values were calculated using $J_{\text{NH-H}\alpha} = A \cos^2|\phi \pm 60^\circ| - B \cos^2|\phi \pm 60^\circ| + C$, where (+) is for a D-confirmation, (-) is for an L-configuration and the values of A, B, C are those proposed by Bystrov et al. for a chiral residue.²² ^b See ref 16 for sandostatin (**I**). ^c This residue is Cys in analog **IV**.

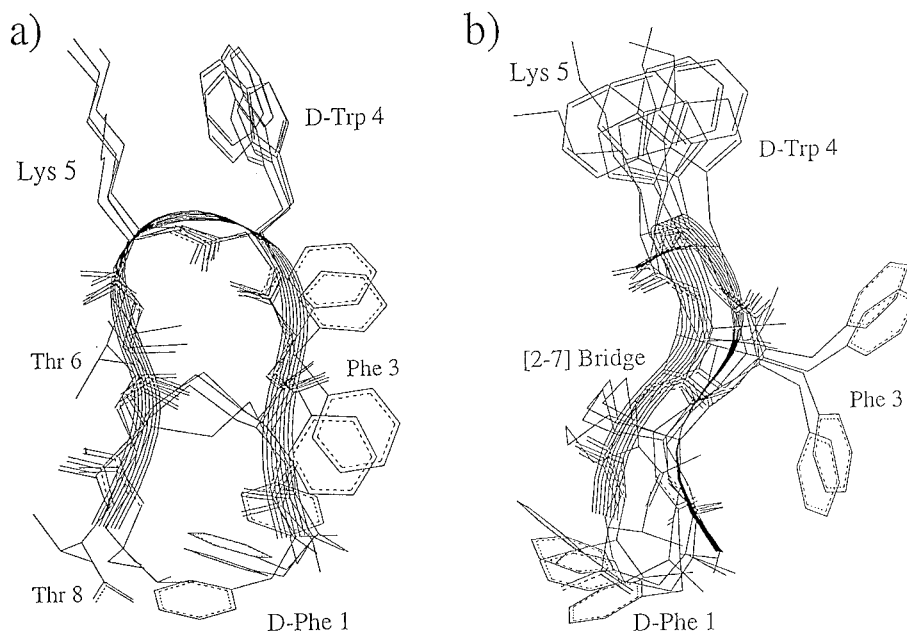


Figure 1. Top (a) and side (b) views of the superimposed structures of compounds **I–V** (Table 1). For the parent molecule sandostatin **I** the backbone of the representative average conformation is shown together with its ribbon diagram. For each conformational cluster of analogs **II–V**, the minimum energy structure is used. All backbones overlay very closely (cf. Table 5), and the χ_1 torsion of the D-Trp⁴ side chain is similar in the analogs considered. Also the χ_1 torsion of the Lys⁵ side chain adopts similar values in the different compounds. The proximity between the aromatic D-Phe¹ side chain and the bridging region is consistent with the observed C_β^2 upfield shifts (see text), but in the ensemble of equilibrating conformations other structures can be present in which the D-Phe¹ side chain is differently arrayed.

Table 4. Temperature Coefficients (–ppb/K) of the Amide Protons^a

residue	II	III	IV	V
Ala ^L ^{2 b}	5.7	8.1	3.6	5.6
Phe ³	4.6	5.2	3.6	5.3
D-Trp ⁴	5.6	5.9	5.0	6.0
Lys ⁵	6.7	4.6	2.6	4.4
Thr ⁶	0.0	0.1	1.6	0.9
Ala ^L ^{7 b}	6.5	6.8	3.6	7.6
Thr ⁸	4.8	4.5		

^a For sandostatin (**I**), see ref 16. ^b This residue is Cys in analog **IV**.

tures, explaining the high-temperature coefficients observed for NH³. It is difficult to evaluate the population of the helix-like ensemble quantitatively, but a qualitative estimate can be obtained using the $J_{\text{NH-H}\alpha}$ coupling constants. Specifically, the average $J_{\text{NH-H}\alpha}$ value for residue 7 computed on the basis of the helix-like conformations is 6.8 Hz¹⁶ while the values measured for analogs **II–V** are consistently higher (Table 3) and closer to those expected for β -sheet-like structures. This observation indicates that the β -sheet-like conformations prevail over the helix-like structures.

Side Chain Conformations. Table 6 shows the χ_1 rotamer populations computed on the basis of the measured $J_{\text{H}\alpha\beta}$ coupling constants using the three-state rotamer model.²¹ The side chain conformations which can be relevant for somatostatin-like binding activity are those of D-Phe¹, D-Trp⁴, and Lys⁵.¹¹ For D-Phe¹, the most populated χ_1 rotamer is consistently the *trans*,

which allows the vicinity between the aromatic group of D-Phe¹ and the bridging region (lanthionine or disulfide; see Figure 1a,b). The presence of conformations in which the aromatic side chain of D-Phe¹ and the bridging region are in close proximity is also consistent with the upfield shift observed for the $C^\beta\text{H}$ protons of residue 2 as compared to the chemical shift of the corresponding protons in the hexamer^{14,29,30} (Table 7). As for the side chains of D-Trp⁴ and Lys⁵, the preferred χ_1 rotamers in the bioactive compounds¹⁴ are *trans* and g^- , respectively, as shown in Table 6. These rotamers allow a close proximity between the side chains of D-Trp⁴ and Lys⁵, which is confirmed by the upfield shift observed for the $C^\gamma\text{H}$ resonances of Lys⁵ (Table 7)³¹ which is caused by the D-Trp⁴ aromatic ring current. These conformational preferences are very similar to those found for the parent compound sandostatin **I**.¹⁶

Refinement of the Model for Somatostatin Pharmacophores. For a proper analysis of the somatostatin pharmacophore, it is important to consider that the peptide backbone is believed to serve primarily as a scaffold to allow for the proper side chain arrangement.¹⁰ The topochemical array of somatostatin analogs is therefore better characterized using the $C^\gamma\text{–}C^\gamma$ distances between side chains rather than the torsion angles.¹¹ Figure 2 shows the $C^\gamma\text{–}C^\gamma$ distances accessible in the previously discussed conformations of sandostatin **I**¹⁶ and in the structures proposed for the lanthionine octamers **II** and **III** and the disulfide heptamer **IV** which bind to the mSSTR2b, rSSTR5, and hSSTR5

Table 5. Backbone to Backbone rmsd^a

compound	II	III	IV	V
⟨sandostatin (I) ^b ⟩	0.636–0.686	0.592–0.796	0.594–1.070 ^c	0.600–0.714

^a All rmsd are reported in angstroms, and the range of computed values is shown. ^b Average sandostatin β -sheet structure. The backbone to backbone rmsd between this structure and those of the β -sheet conformational cluster obtained for sandostatin is only 0.489 ± 0.139 Å.¹⁶ ^c The standard deviations of the backbone torsions of analog **IV** are all smaller than 30°.

Table 6. The $J_{\text{H}\alpha\beta}$ Coupling Constants and the Calculated Side Chain Populations^a

residue	II		III		IV		V	
	$J_{\alpha-\beta}, J_{\alpha-\beta\text{H}}$	(t, g ⁻ , g ⁺)	$J_{\alpha-\beta}, J_{\alpha-\beta\text{H}}$	(t, g ⁻ , g ⁺)	$J_{\alpha-\beta}, J_{\alpha-\beta\text{H}}$	(t, g ⁻ , g ⁺)	$J_{\alpha-\beta}, J_{\alpha-\beta\text{H}}$	(t, g ⁻ , g ⁺)
D-Phe ¹	5.54	0.47	4.18	0.52	5.58	0.47	5.50	0.44
	8.39	0.34	8.86	0.42	8.39	0.33	8.16	0.37
Ala _L ^{2 b}		0.19		0.06		0.20		0.19
	5.03	0.22	6.33	0.34			7.14	0.41
	7.55	0.45	8.19	0.51			7.88	0.48
Phe ³		0.33		0.15				0.11
	6.67	0.30	6.52	0.29	9.15	0.38	6.87	0.32
	7.27	0.36	6.52	0.27	7.40	0.54	7.51	0.39
D-Trp ⁴		0.34		0.44				0.29
	7.75	0.41	7.17	0.43	8.39	0.47	7.05	0.34
	7.15	0.24	7.96	0.22	7.46	0.15	7.51	0.28
Lys ⁵		0.35		0.35				0.38
	4.42	0.16	3.83	0.11	4.30	0.15	4.41	0.16
	10.97	0.76	11.17	0.78	~11	0.77	10.70	0.73
Thr ⁶		0.08		0.11				0.11
	4.77	0.19 ^c	4.69	0.19 ^c	5.58	0.27 ^c	4.92	0.21 ^c
	5.45	0.26	6.52	0.36	4.60	0.18	4.58	0.33
Ala _L ^{7 b}		0.43		0.48				0.17
	7.27	0.31	7.92	0.16	9.37	0.62	6.32	0.17
		0.30 ^c	4.84	0.20 ^c		0.20		0.50

^a Values were calculated using $J_{\text{T}} = 13.56$ and $J_{\text{G}} = 2.60$ Hz for nonaromatic side chains, $J_{\text{T}} = 13.85$ and $J_{\text{G}} = 3.55$ Hz for aromatic side chains.²¹ The sandostatin (I), see ref 16. ^b This residue is Cys in analog IV. ^c These values refer to the g⁻ rotamer.

Table 7. Chemical Shifts^a

residue	(δ in ppm)	II	III	IV	V	
D-Phe	α	4.13	4.12	4.15	4.10	
	β	2.91, 3.12	2.91, 3.12	2.93, 3.11	2.93, 3.10	
	others	(o) 7.30, (m) 7.35 (p) 7.32	(o) 7.31, (m) 7.39 (p) 7.33	(o) 7.26, (m) 7.30 (p) 7.30	(o) 7.31, (m) 7.31 (p) 7.31	
Ala _L ^{2 b}	NH	8.80	8.84	8.78	8.76	
	α	4.71	4.85	4.86	4.70	
	β	2.55, 2.78	2.58, 2.76	2.82, 2.82	2.55, 2.71	
Phe ³	NH	8.22	8.25	8.37	8.26	
	α	4.65	4.64	4.67	4.65	
	β	2.73, 2.86	2.74, 2.85	2.75, 2.83	2.87, 2.87	
others	(o) 6.98, (m) 7.11 (p) 7.03	(o) 6.96, (m) 7.06 (p) 7.00	(o) 7.04, (m) 7.15 (p) 7.06	(o) 7.00, (m) 7.13 (p) 7.06		
	D-Trp ⁴	NH	8.43	8.48	8.64	8.45
		α	4.38	4.36	4.20	4.38
β		2.79, 2.99	2.76, 2.97	2.75, 2.94	2.79, 3.01	
H1,H2		10.82, 7.08	10.80, 7.05	10.76, 6.97	10.80, 7.05	
	H4,H5	7.54, 6.99	7.51, 7.00	7.43, 6.98	7.54, 7.02	
	H6,H7	7.09, 7.33	7.06, 7.33	7.06, 7.30	7.09, 7.33	
Lys ⁵	NH	8.49	8.46	8.39	8.34	
	α	4.00	3.99	3.93	4.02	
	β	1.45, 1.65	1.37, 1.64	1.31, 1.68	1.37, 1.66	
γ, δ		0.96, 1.38	0.93, 1.36	0.82, 1.31	0.96, 1.38	
	Thr ⁶	$\epsilon, \text{NH}\epsilon$	2.63, 7.34	2.60, 7.65	2.56, 7.61	—, —
		NH	7.39	7.39	7.67	7.45
α		4.22	4.29	4.29	4.20	
β		4.03	4.00	4.11	4.04	
	γ	1.03	1.02	1.08	1.04	
	OH	5.01	4.91	4.82	4.83	
Ala _L ^{7 b}	NH	7.92	8.07	8.34	7.99	
	α	4.66	4.76	4.75	4.60	
	β	2.62, 2.92	2.58, 2.90	2.84, 3.03	2.67, 2.96	
Thr ^{8 c}	NH	7.26	7.69			
	α	3.61	4.16			
	β	3.91	4.00			
	γ	1.05	1.02			
	OH	4.70	4.93			

^a DMSO- d_6 solution, 300 K. For sandostatin (I), see ref 16. ^b This residue is Cys in analog IV. ^c The resonances of the CH₂OH group of the lanthionine octamer-ol (II) are at 3.30 and 3.43 ppm (CH₂) and 4.60 ppm (OH).

receptors in the nanomolar range (Table 1).¹⁴ The resulting topology is similar to that of the model independently proposed for the binding to somatostatin receptors on the basis of α - and β -methylation studies (Figure 2).¹¹

The C γ -C γ distances accessible to sandostatin I and to its bioactive analogs II-IV (Table 1 and Figure 2) are consistent with those of the pharmacophore model

based on α - and β -methylated compounds (distances in parentheses in Figure 2),¹¹ except for the C γ -C γ distance between residues D-Phe¹ and D-Trp⁴ and between residues D-Phe¹ and Lys⁵. In the octamers I-III and in the heptamer IV these distances are at least 3 Å longer than the corresponding distances in the model based on the α - and β -methylated analogs of compound L-363-301 (Figure 2).¹¹ This variation in distances can

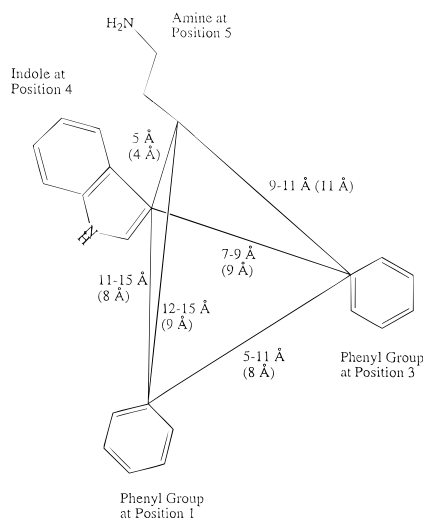


Figure 2. Side chain-side chain $C^\gamma-C^\gamma$ distances accessible to sandostatin **I** and to the bioactive lanthionine octamers **II**, **III** and disulfide heptamer **IV**. The distances reported in parantheses refer to the pharmacophore model based on the α - and β -methylated analog series.¹¹

be explained considering the presence of the disulfide bridge in sandostatin **I**, which can occupy the same position relative to the D-Trp⁴ and Lys⁵ side chains as the side chain of Phe⁷ in the α - and β -methylated analogs of compound L-363-301. Thus the disulfide bridge may assist the interaction with SSTR2 receptors. These observations on the importance of the disulfide bridge for receptor binding are fully consistent with the high bioactivity of the disulfide and backbone-to-backbone bicyclic somatostatin analog c[Cys-Phe-D-Trp-Lys-Thr-Cys] in which the disulfide replaces the aromatic moiety corresponding to the Phe⁷ of the α - and β -methylated analogs³² (Phe¹¹ in the numbering of ref 32).

Additional features of the role of the disulfide group in somatostatin binding activity are revealed by the lanthionine octamer analogs **II** and **III**. As discussed above, both of these compounds show conformational preferences similar to those observed for sandostatin **I**. In addition, they maintain binding potencies at the mSSTR2b, rSSTR5, and hSSTR5 receptors in the nanomolar range¹⁴ (Table 1), suggesting that the lanthionine group is a good mimetic of the disulfide bridge. The monosulfide octamers **II** and **III** bind to mSSTR2b receptors with IC_{50} values greater than those measured for sandostatin **I** (Table 1), consistent with the above-mentioned interaction between these type of receptors and the disulfide bridge. On the other hand, the binding affinity for the rSSTR5 receptor is less affected by the replacement of the disulfide with a monosulfide bridge (Table 1), resulting in increased mSSTR2b/rSSTR5 selectivities for the lanthionine octamers **II** and **III** as compared to sandostatin **I**.¹⁴

Information about the biological role of Thr⁸ is provided by the disulfide heptamer (**IV**). As seen above, this compound shows conformational preferences common to sandostatin **I**, explaining its nanomolar binding affinity for the mSSTR2b, rSSTR5, and hSSTR5 somatostatin receptors (Table 1). However, similar to the lanthionine octamers **II** and **III**, the disulfide heptamer **IV** binds to these receptors with IC_{50} values greater than those measured for sandostatin **I** (Table 1), suggesting that Thr⁸-ol may still affect the interaction with

the mSSTR2b, rSSTR5, and hSSTR5 receptors. This conclusion is fully consistent with the inactivity of the lanthionine heptamer (**V**, Table 1) in which the affinity promoting Thr⁸-ol and disulfide groups are both absent.

Conclusions

The conformational analysis of lanthionine and disulfide analogs of sandostatin has allowed us to reveal pharmacophore features consistent with the model for binding activity independently proposed in our laboratory on the basis of α - and β -methylation studies.¹¹ In addition, we have shown that the disulfide bridge between residues 2 and 7 may be involved in interactions with the SSTR2 receptor. This finding is in full agreement with the results of Veber et al. which demonstrated that a disulfide can replace an aromatic moiety in key somatostatin receptor-ligand interactions.³² Replacement of the disulfide with a monosulfide lanthionine bridge affects the binding to mSSTR2b receptors and leads to increased mSSTR2b/rSSTR5 selectivities.

We also give insight into the role of Thr in position 8 showing that, although this residue can stabilize β -sheet-like structures through intramolecular hydrogen bonding,¹² the absence of Thr⁸-ol or Thr⁸-NH₂ does not preclude the accessibility to β -sheet-like conformations of the hexapeptide ring. Furthermore, our studies suggest that Thr⁸-ol can affect the interactions with the somatostatin mSSTR2b, rSSTR5, and hSSTR5 receptors, even though Thr⁸ is not essential for the binding to these receptors as demonstrated by the binding potencies of the disulfide heptamer **IV** in which Thr⁸-ol is missing.

This work also provides new information on the structural properties of the lanthionine hexapeptide ring, showing that the lanthionine moiety is a good mimetic of β -VI turns. These conclusions together with the results on the effect of the disulfide bridge and of Thr⁸ are significant for the design of novel bioactive sandostatin analogs.

Abbreviations. Ala_L, each of the lanthionine amino acid ends linked by the monosulfide bridge; DG, distance geometry; DMSO-*d*₆, fully deuterated dimethyl sulfoxide; DQF-COSY, double quantum-filtered correlation spectroscopy; gauche (-), *g*⁻; gauche (+), *g*⁺; $J_{H\alpha\beta}$, coupling constant between the C^αH and the C^βH protons; $J_{NH-H\alpha}$, coupling constant between the NH and the C^αH protons; MD, molecular dynamics; NOE, nuclear overhauser enhancement; NMR, nuclear magnetic resonance; rmsd, root mean square deviation; ROESY, rotating frame nuclear overhauser spectroscopy; TOCSY, total correlation spectroscopy.

Acknowledgment. This research was supported by the NIH-DK 15410 Grant. We are grateful to Noriyuki Kawahata, Dr. Ralph-Heiko Mattern, and Dr. Kevin Shreder for stimulating and helpful discussion. We also thank Mr. J. P. Taulane for his careful technical assistance.

References

- Brazeau, P.; Vale, W.; Burgus, R.; Ling, N.; Bucher, M.; Rivier, J.; Guillemin, R. Hypothalamic Polypeptide That Inhibits the Secretion of the Immunoreactive Growth Hormone. *Science* **1973**, *179*, 77-79.
- Koerker, D. J.; Harker, L. A.; Goddner, C. J. N. Effects of Somatostatin on Hemostasis in Baboons. *N. Engl. J. Med.* **1975**, *293*, 476-479.

- (3) Gerich, J. E.; Lovinger, R.; Grodsky, G. M. Inhibition by Somatostatin of Glucagon and Insulin Release from the Perfused Rat Pancreas in Response to Arginine, Isoproterenol and Theophylline: Evidence for a Preferential Effect on Glucagon Secretion. *Endocrinology* **1975**, *96*, 749–754.
- (4) Johansson, C.; Wisen, O.; Efendic, S.; Uvnas-Wallensten, K. Effects of Somatostatin on Gastrointestinal Propagation and Absorption of Oral Glucose in Man. *Digestion* **1981**, *22*, 126–137.
- (5) Iverson, L. L. Nonopioid Neuropeptides in Mammalian CNS. *Annu. Rev. Pharmacol. Toxicol.* **1983**, *23*, 1–27.
- (6) Delfs, J. R.; Dichter, M. A. Effects of Somatostatin on Mammalian Cortical Neurons in Culture: Physiological Actions and Unusual Dose Response Characteristics. *J. Neurosci.* **1983**, *3* (6), 1176–1188.
- (7) Epelbaum, J. Somatostatin in the Central Nervous System: Physiology and Pathological Modifications. *Prog. Neurobiol.* **1986**, *27*, 63–100.
- (8) Seybold, V. S.; Hylden, J. L. K.; Wilcox, G. L. Intrathecal Substance P and Somatostatin in Rats: Behaviors Indicative of Sensation. *Peptides* **1982**, *3* (1), 49–54.
- (9) Veber, D. F.; Freidinger, R. M.; Perlow, D. S.; Paleveda, W. J., Jr.; Holly, F. W.; Strachan, R. G.; Nutt, R. F.; Arison, B. J.; Homnick, C.; Randall, W. C.; Glitzer, M. S.; Saperstein, R.; Hirschmann, R. A Potent Cyclic Hexapeptide Analogue of Somatostatin. *Nature* **1981**, *292*, 55–58.
- (10) Mierke, D. F.; Pattaroni, C.; Delaet, N.; Toy, A.; Goodman, M.; Tancredi, T.; Motta, A.; Temussi, P. A.; Moroder, L.; Bovermann, G.; Wunsch, E. Cyclic Hexapeptides Related to Somatostatin. *Int. J. Pept. Protein Res.* **1990**, *36*, 418–432.
- (11) (a) Huang, Z.; He, Y.-B.; Raynor, K.; Tallent, M.; Reisine, T.; Goodman, M. Main Chain and Side Chain Chiral Methylated Somatostatin Analogs: Synthesis and Conformational Analysis. *J. Am. Chem. Soc.* **1992**, *114* (24), 9390–9401. (b) He, Y.-B.; Huang, Z.; Raynor, K.; Reisine, T.; Goodman, M. Synthesis and Conformations of Somatostatin Related Cyclic Hexapeptides Incorporating Specific α -Methylated and β -Methylated Residues. *J. Am. Chem. Soc.* **1993**, *115*, 8066–8072.
- (12) Bauer, W.; Briner, U.; Doepfner, W.; Haller, R.; Huguenin, R.; Merbach, P.; Petcher, T. J.; Pless, J. SMS 201-995: A Very Potent and Selective Octapeptide Analogue of Somatostatin with Prolonged Action. *Life Sci.* **1982**, *31*, 1133–1140.
- (13) Van Binst, G.; Tourwe, D. Backbone Modifications in Somatostatin Analogues: Relation Between Conformation and Activity. *Peptide Res.* **1992**, *5* (1), 8–13.
- (14) Ósapay, G.; Prokai, L.; Kim, H. S.; Medzihradsky, K. F.; Coy, D. H.; Liapakis, G.; Reisine, T.; Melacini, G.; Zhu, Q.; Wang, S. H.-H.; Goodman, M. Lanthionine–Somatostatin Analogs: Synthesis, Characterization, Biological Activity and Enzymatic Stability Studies. *J. Med. Chem.* **1997**, *40*, 2241–2251.
- (15) Jung, G. Peptides with Sulfide Bridges and Dehydroamino Acids: Their Prepropeptides and Possibilities for Bioengineering. In *Peptides. Proceedings of the Eleventh American Peptide Symposium*; Rivier, J., Marshall, G. R., Eds.; ESCOM: Leiden, 1990; pp 865–869.
- (16) Melacini, G.; Zhu, Q.; Goodman, M. Multiconformational NMR Analysis of Sandostatin (Octreotide): Equilibrium between β -Sheet and Helical Structures. *Biochemistry* **1997**, *36*, 1233–1241.
- (17) (a) Aue, W. P.; Bartholdi, E.; Ernst, R. R. Two-Dimensional Spectroscopy. Application to Nuclear Magnetic Resonance. *J. Chem. Phys.* **1976**, *64*, 2229–2246. (b) Bodenhausen, G.; Vold, R. L.; Vold, R. R. Multiple Quantum Spin-Echo Spectroscopy. *J. Magn. Reson.* **1980**, *B37*, 93–106. (c) Bax, A.; Freeman, R. Investigations of Complex Networks of Spin-Spin Coupling by Two-Dimensional NMR. *J. Magn. Reson.* **1981**, *44*, 542–561.
- (18) (a) Rance, M.; Sorensen, O. W.; Bodenhausen, G.; Wagner, G.; Ernst, R. R.; Wuthrich, K. Improved Spectra Resolution in Cosy ^1H -NMR Spectra of Proteins via Double Quantum Filters. *Biochem. Biophys. Res. Commun.* **1984**, *117*, 479–485. (b) Davis, D.; Bax, A. Assignment of Complex ^1H -NMR Spectra via Two-Dimensional Homonuclear Hartmann-Hahn Spectroscopy. *J. Am. Chem. Soc.* **1985**, *107*, 2820–2821.
- (19) Bothner-By, A. A.; Stephens, R. L.; Lee, J.; Warren, C. D.; Jeanloz, R. W. Structure Determination of a Tetrasaccharide: Transient Nuclear Overhauser Effects in the Rotating Frame. *J. Am. Chem. Soc.* **1984**, *106*, 811–813.
- (20) Wüthrich, K. *NMR of Proteins and Nucleic Acids*; Wiley: New York, 1986.
- (21) (a) Yamazaki, T.; Probstl, A.; Schiller, P. W.; Goodman, M. Biological and Conformational Studies of [Val⁴]-Morphiceptin and [D-Val⁴]-Morphiceptin Analogs Incorporating Cis-2-Aminocyclopentane Carboxylic Acid as Peptidomimetic for Proline. *Int. J. Pept. Protein Res.* **1991**, *37*, 364–381. (b) Pachler, K. G. P. Nuclear Magnetic Resonance Study of Some α -Amino Acids-II. Rotational Isomerism. *Spectrochim. Acta* **1964**, *20*, 581–587. (c) Cung, M. T.; Marraud, M. Conformational Dependence of the Vicinal Proton Coupling Constant for the C $^{\alpha}$ –C $^{\beta}$ Bond in Peptides. *Biopolymers* **1982**, *21*, 953–967.
- (22) Bystrov, V. F.; Ivanov, V. T.; Portnova, S. L.; Blashova, T. A.; Ovchinnikov, Y. A. Refinement of the Angular Dependence of the Peptide Vicinal NH-C $^{\alpha}$ H Coupling Constant. *Tetrahedron* **1973**, *29*, 873–877.
- (23) Kessler, H. Conformation and Biological Activity of Cyclic Peptides. *Angew. Chem., Int. Ed. Engl.* **1982**, *21*, 512–523.
- (24) Biosym/MSI, Inc.
- (25) McCammon, J. A.; Wolynes, P. G.; Karplus, M. Picosecond Dynamics of Tyrosine Side Chains in Proteins. *Biochemistry* **1979**, *18* (6), 927–942.
- (26) Kazmierski, W. M.; Ferguson, R. D.; Lipkowski, A. W.; Hruby, V. J. A Topographical Model of μ -Opioid and Brain Somatostatin Receptor Selective Ligands. *Int. J. Pept. Protein Res.* **1995**, *46*, 265–278.
- (27) Polinsky, A.; Cooney, M. G.; Toy-Palmer, A.; Ósapay, G.; Goodman, M. Synthesis and Conformational Properties of the Lanthionine-Bridged Opioid Peptide [D-AlaL2,AlaL5] Enkephalin as Determined by NMR and Computer Simulations. *J. Med. Chem.* **1992**, *35*, 4185–4194.
- (28) For temperature coefficients between 2 and 4 ppb/K no reliable information on solvent shielding can be obtained.²³ This is the case for the temperature coefficients of the NH², NH³, NH⁵, and NH⁷ resonances of the disulfide heptamer **IV** (Table 4).
- (29) Wynants, C.; Van Binst, G.; Loosli, H. R. Hexapeptide Analogue of Somatostatin, Sandoz 201–456; Conformational Study in Dimethylsulfoxide by 1D and 2D NMR Methods. *Int. J. Pept. Protein Res.* **1985**, *25*, 622–627.
- (30) For the analogs incorporating the lanthionine bridge (**II**, **III**, and **V** in Table 1), the reference chemical shift for the C $^{\beta}$ H protons of residue 2 are those of the lanthionine bridged hexamer¹⁴ [Ala^{1,2}-Phe^{3,D}-Trp⁴-Lys⁵-Thr⁶-Ala⁷] both at 2.96 ppm. For the analog with the disulfide bridged (heptamer **IV** of Table 1), the reference chemical shift for the C $^{\beta}$ H protons of residue 2 are those of the disulfide-bridged hexamer [Cys²-Phe^{3,D}-Trp⁴-Lys⁵-Thr⁶-Cys⁷]-NH₂ at 2.99 and 3.23 ppm.²⁹
- (31) Wynants, C.; Van Binst, G.; Loosli, H. R. SMS 201–995, An Octapeptide Somatostatin Analogue; Assignments of the ^1H 500 MHz NMR Spectra and Conformational Analysis of SMS 201–995 in Dimethylsulfoxide. *Int. J. Pept. Protein Res.* **1985**, *25*, 615–621.
- (32) Brady, S. F.; Paleveda, W. J.; Arison, B. H.; Saperstein, R.; Brady, E. J.; Raynor, K.; Reisine, T.; Veber, D. F.; Freidinger, R. M. Approaches to Peptidomimetics which Serve as Surrogates for the *cis* Amide Bond: Novel Disulfide-Constrained Bicyclic Hexapeptide Analogs of Somatostatin. *Tetrahedron* **1993**, *49* (17), 3449–3466.

JM960851A